2009

Functional Interaction between the Fanconi Anemia D2 Protein and Proliferating Cell Nuclear Antigen (PCNA) via a Conserved Putative PCNA Interaction Motif

Niall G. Howlett
University of Rhode Island, nhowlett@uri.edu

Julie A. Harney
University of Rhode Island

Meghan A. Rego
University of Rhode Island

Frederick W. Kolling IV
University of Rhode Island

Thomas W. Glover

Citation/Publisher Attribution

Howlett, N. G., Harney, J. A., Rego, M. A., Kolling, F. W., IV. (2009). Functional Interaction between the Fanconi Anemia D2 Protein and Proliferating Cell Nuclear Antigen (PCNA) via a Conserved Putative PCNA Interaction Motif. *Journal of Biological Chemistry, 284*, 28935-28942. doi: 10.1074/jbc.M109.016352
Available at: http://dx.doi.org/10.1074/jbc.M109.016352

Functional Interaction between the Fanconi Anemia D2 Protein and Proliferating Cell Nuclear Antigen (PCNA) via a Conserved Putative PCNA Interaction Motif

THE JOURNAL OF BIOLOGICAL CHEMISTRY VOL. 284, NO. 42, pp. 28935–28942, October 16, 2009

Functional Interaction between the Fanconi Anemia D2 Protein and Proliferating Cell Nuclear Antigen (PCNA) via a Conserved Putative PCNA Interaction Motif*[S]

Received for publication, May 22, 2009, and in revised form, August 24, 2009 Published, JBC Papers in Press, August 24, 2009, DOI 10.1074/jbc.M109.016352

Niall G. Howlett[‡1], **Julie A. Harney**[‡], **Meghan A. Rego**[‡], **Frederick W. Kolling IV**[‡], **and Thomas W. Glover**[§¶]

From the [‡]*Department of Cell and Molecular Biology, University of Rhode Island, Kingston, Rhode Island 02881 and the Departments of* [§]*Human Genetics and* [¶]*Pediatrics, University of Michigan, Ann Arbor, Michigan 48109*

Fanconi Anemia (FA) is a rare recessive disease characterized by congenital abnormalities, bone marrow failure, and cancer susceptibility. The FA proteins and the familial breast cancer susceptibility gene products, BRCA1 and FANCD1/BRCA2, function cooperatively in the FA-BRCA pathway to repair damaged DNA and to prevent cellular transformation. Activation of this pathway occurs via the mono-ubiquitination of the FANCD2 protein, targeting it to nuclear foci where it co-localizes with FANCD1/BRCA2, RAD51, and PCNA. The regulation of the mono-ubiquitination of FANCD2, as well as its function in DNA repair remain poorly understood. In this study, we have further characterized the interaction between the FANCD2 and PCNA proteins. We have identified a highly conserved, putative FANCD2 PCNA interaction motif (PIP-box), and demonstrate that mutation of this motif disrupts FANCD2-PCNA binding and precludes the mono-ubiquitination of FANCD2. Consequently, the FANCD2 PIP-box mutant protein fails to correct the mitomycin C hypersensitivity of FA-D2 patient cells. Our results suggest that PCNA may function as a molecular platform to facilitate the mono-ubiquitination of FANCD2 and activation of the FA-BRCA pathway.

Fanconi anemia (FA)[2] is a rare recessive disorder characterized by developmental abnormalities, progressive bone marrow failure, and pronounced cancer susceptibility (1). FA patients are particularly susceptible to early-onset acute myelogenous leukemia and squamous cell carcinoma of the head, neck, and gynecologic regions (2). FA patient cells are hypersensitive to the clastogenic effects of DNA cross-linking agents, *e.g.* mitomycin C (MMC), and agents that inhibit DNA replication, *e.g.* aphidicolin (APH) (3, 4). There are currently thirteen genetically defined FA complementation groups (A, B, C, D1, D2, E, F, G, I, J, L, M, and N), and all thirteen genes have been identified (5).

A central step in the activation of the FA-BRCA pathway is the mono-ubiquitination of the FANCD2 and FANCI proteins, catalyzed by the core FA E2/E3 holoenzyme complex (5, 6). The mono-ubiquitination of FANCD2 and FANCI signals their translocation to discrete nuclear foci, where they co-localize with the BRCA1 and RAD51 DNA repair proteins, as well as the major cellular DNA polymerase processivity factor PCNA (3, 4, 7–9). Several studies have suggested an important role for the FA-BRCA pathway in a DNA replication-associated DNA repair process, *e.g.* homologous recombination (HR), and/or translesion DNA synthesis (TLS) (3, 4, 10–12). Accordingly, additional proteins with established roles in the DNA replication stress response, including ATR, CHK1, HCLK2, and RPA, modulate DNA damage-inducible FANCD2 mono-ubiquitination (13–15). Our understanding of the regulation of this critical post-translational modification, however, is incomplete.

We, and others (4, 7) have previously reported an association between FANCD2 and PCNA. FANCD2 and PCNA co-localize in nuclear foci following treatment with agents that inhibit DNA replication. Like FANCD2, PCNA is mono-ubiquitinated following exposure to DNA-damaging agents (16, 17). While FANCD2 and PCNA are mono-ubiquitinated by different E3 ubiquitin ligases, FANCL and RAD18 (16–19), respectively, both proteins are de-ubiquitinated by the USP1 enzyme (20, 21). The functional significance of the FANCD2-PCNA interaction, however, has not been determined.

In addition to its role as a DNA polymerase processivity factor, PCNA interacts with many DNA repair proteins, *e.g.* MSH3, XPG, and $p21^{Cip1/Waf1}$ (22). These interactions typically occur in a hydrophobic pocket of the PCNA homotrimer, termed the interdomain connecting loop (ICL). Proteins that interact with the PCNA ICL harbor a highly conserved PCNA-binding motif called the PIP-box, defined by the amino acid sequence Q*XX*h*XX*aa, where h represents amino acids with moderately hydrophobic side chains, *e.g.* leucine, isoleucine, or methionine (L, I, M), a represents amino acids with highly hydrophobic, aromatic side chains, *e.g.* phenylalanine and tyrosine (F, Y), and *X* is any amino acid (23).

Here, we describe an important functional interaction between FANCD2 and PCNA. We have identified a highly con-

* This work was supported, in whole or in part, by National Institutes of Health Grant R01CA043222-21 (to T. W. G.). This work was also supported by a Fanconi Anemia Research Foundation grant (to N. G. H. and T. W. G.), a Leukemia Research Foundation New Investigator grant (to N. G. H.), and a RI-INBRE Grant P20RR016457-09 from the National Center for Research Resources.

[S] The on-line version of this article (available at http://www.jbc.org) contains supplemental Figs. S1 and S2.

[1] To whom correspondence should be addressed: 379 CBLS, 120 Flagg Rd., Kingston, RI 02881. Tel.: 401-874-4306; Fax: 401-874-2065; E-mail: nhowlett@mail.uri.edu.

[2] The abbreviations used are: FA, Fanconi anemia; APH, aphidicolin; FA-D2, Fanconi anemia complementation group D2; FANCD2, Fanconi anemia D2 protein; GST, glutathione *S*-transferase; HR, homologous recombination; IF, immunofluorescence microscopy; MMC, mitomycin C; PCNA, proliferating cell nuclear antigen; PIP-box, PCNA-interaction motif; TLS, translesion DNA synthesis; MOPS, 4-morpholinepropanesulfonic acid; HA, hemagglutinin; WCE, whole cell extract; wt, wild type.

served putative PIP-box in FANCD2, and demonstrate that mutation of this motif disrupts the FANCD2-PCNA interaction, and precludes both the spontaneous and DNA damage-inducible mono-ubiquitination of FANCD2. Consequently, the FANCD2 PIP-box mutant fails to correct the MMC hypersensitivity of FA-D2 patient-derived cells. However, the mutant protein retains the ability to localize to chromatin, interact with FANCE, and undergo DNA damage-inducible phosphorylation. Our results suggest that PCNA may act as a molecular platform for the mono-ubiquitination of FANCD2 and for the activation of the FA-BRCA pathway.

EXPERIMENTAL PROCEDURES

Cell Culture, Plasmids, and Site-directed Mutagenesis—COS-7, PD20F, and HCT116 cells were grown in Dulbecco's modified Eagle's medium (DMEM) supplemented with 12% (v/v) fetal bovine serum. PD20F pMMP-FANCD2 cells were maintained in DMEM supplemented with 1 μg/ml puromycin. PD20F plus 6xHis/V5-FANCD2 were maintained in DMEM supplemented with 200 μg/ml G418. The *FANCD2 PIP*Δ cDNA was generated by site-directed mutagenesis of the wild-type *FANCD2* cDNA by PCR-based site-directed mutagenesis using 74-mer forward and reverse oligonucleotides, containing a total of 8 mismatches (underlined): CAG CAA ATA CGA AAA CTC TTC TAT ← GCG CAA ATA GCA AAA CTC GCC GCT. pDEST40 (Invitrogen) is a pcDNA3-based plasmid for the expression of C terminus 6xHis/V5 fusion proteins. pMT5-FLAG-p21 (Addgene) is an N terminus FLAG-tagged p21 mammalian expression vector.

Immunoblotting and Immunoprecipitations—Whole-cell extracts (WCE) for immunoblotting were prepared by lysis of cells in 2% SDS lysis buffer with boiling. For immunoprecipitations (IP), lysates were prepared in radioimmune precipitation assay buffer or NETN buffers supplemented with protease and phosphatase inhibitors (24). Between 400 and 1000 μg of total protein were used per IP reaction. For the Ni^{2+} pull-down experiments, whole-cell lysates were prepared in 50 mM Tris, pH 7.8, 300 mM NaCl, 10 mM imidazole, 0.5% (v/v) Nonidet P-40, supplemented with protease and phosphatase inhibitors, and incubated with Ni^{2+} beads for 1 h at 4 °C. The GST pull-down experiments were performed as previously described (25), and whole-cell lysates were incubated with 10 μg of recombinant GST-Empty or GST-PCNA for 1 h at 4 °C. Proteins were resolved using NuPAGE 3–8% (w/v) Tris-acetate or 4–12% (w/v) Bis-Tris (MOPS) gels (Invitrogen). The following antibodies were used: rabbit polyclonal antisera against FANCD2 (NB100–182, Novus Biologicals), PCNA (FL-261; Santa Cruz Biotechnology), FLAG (F7425; Sigma), and histone H2A (acidic patch) (07-146, Millipore), and mouse monoclonal sera against DNA polymerase δ catalytic subunit (610972; BD Biosciences), FANCD2 (FI-17; Santa Cruz Biotechnology), PCNA (PC10; Santa Cruz Biotechnology), α-tubulin (MS-581-PO, Neomarkers), and V5 (Invitrogen). Images were analyzed, and band intensities quantified using ImageJ.

λ *Phosphatase Treatment*—Cells were lysed in modified λ phosphatase reaction buffer (50 mM Tris-HCl, pH 7.5, 150 mM NaCl, 0.1 mM EGTA, 2 mM dithiothreitol, 2 mM $MnCl_2$, 0.01% (v/v) Brij 35, 0.5% (v/v) Nonidet P-40) supplemented with protease inhibitors, with sonication for 10 s. Approximately 10 units of λ phosphatase per μg of protein were incubated at 30 °C for 1 h, prior to loading.

Cellular Subfractionation and Immunocytochemistry—Cells were grown in 15-cm^2 dishes, incubated in the absence or presence of 120 nM MMC for 24 h, washed with phosphate-buffered saline, and harvested in S1 hypotonic lysis buffer (10 mM Tris-HCl, pH 7.4, 10 mM KCl, 1.5 mM $MgCl_2$, 10 mM β-mercaptoethanol). Nuclear soluble proteins (S2 fraction) were extracted with a high-salt buffer (15 mM Tris-HCl, pH 7.4, 1 mM EDTA, 500 mM NaCl, 1 mM $MgCl_2$, 10% glycerol, 10 mM β-mercaptoethanol, plus protease inhibitors). To enrich for chromatin-associated proteins, salt-extracted pellets were treated with 3 units/μl of micrococcal nuclease for 20 min at room temperature in nuclease reaction buffer (20 mM Tris-HCl, pH 7.4, 100 mM KCl, 2 mM $MgCl_2$, 1 mM $CaCl_2$, 0.3 M sucrose, 0.1% Triton X-100, plus protease inhibitors). FANCD2 immunocytochemistry was performed as described previously (3, 4).

DNA Damage Assays—MMC sensitivity and chromosome breakage assays were performed as described previously (4, 26). Statistical analysis of total chromosome gaps and breaks data were carried out using the Student's *t*-test for equal or unequal variance. Variance for each data set was determined using the sample variance F-test. Cells were X-irradiated using a Philips 250 orthovoltage unit at ~2 Gy/min in the Irradiation Core of the University of Michigan Cancer Center.

RESULTS

Further Characterization of the FANCD2-PCNA Interaction—Using immunoprecipitation approaches, we sought to expand upon previous findings of an association between FANCD2 and PCNA in DNA damage-inducible nuclear foci (4, 7). First, whole-cell lysates were prepared from HeLa cells stably expressing HA-tagged PCNA, untransfected or transiently transfected with a positive control FLAG-tagged p21 construct. HA-PCNA co-immunoprecipitated with FLAG-p21 as well as both non- and mono-ubiquitinated FANCD2 (Fig. 1*A*). Next, we generated a FA-D2 (FANCD2-null) patient cell line stably expressing 6xHis/V5-tagged FANCD2 (Fig. 1*B*). Expression of 6xHis/V5-FANCD2 rescued the MMC hypersensitivity of these cells (results not shown). Using a Ni-nitrilotriacetic acid pull-down approach, endogenous PCNA co-immunoprecipitated with 6xHis/V5-FANCD2 from these cells (Fig. 1*B*, *lower panel*, *lane 3*). To analyze the interaction between endogenous FANCD2 and PCNA in chromatin, HCT116 cells were irradiated with 40 J/m^2 UV-C, fractionated in low and high salt lysis buffers, and sonicated briefly to release chromatin-bound proteins (24). We observed an enrichment for mono-ubiquitinated FANCD2 in the sonicated high salt cellular fraction, as expected (27) (Fig. 1*C*, *upper panel*, *lanes 3* and *6*). A mouse monoclonal anti-PCNA antibody, but not mouse IgG, exclusively co-immunoprecipitated FANCD2 from both high salt fractions (Fig. 1*C*, *middle panel*, *lanes 5* and *6*). The specificity of the anti-PCNA mouse monoclonal antibody for PCNA immune complexes was confirmed by immunoblotting with an anti-PCNA rabbit polyclonal antibody (Fig. 1*C*, *lower panel*). In a reciprocal approach, a rabbit polyclonal anti-FANCD2 antibody, but not rabbit serum, preferentially immunoprecipitated

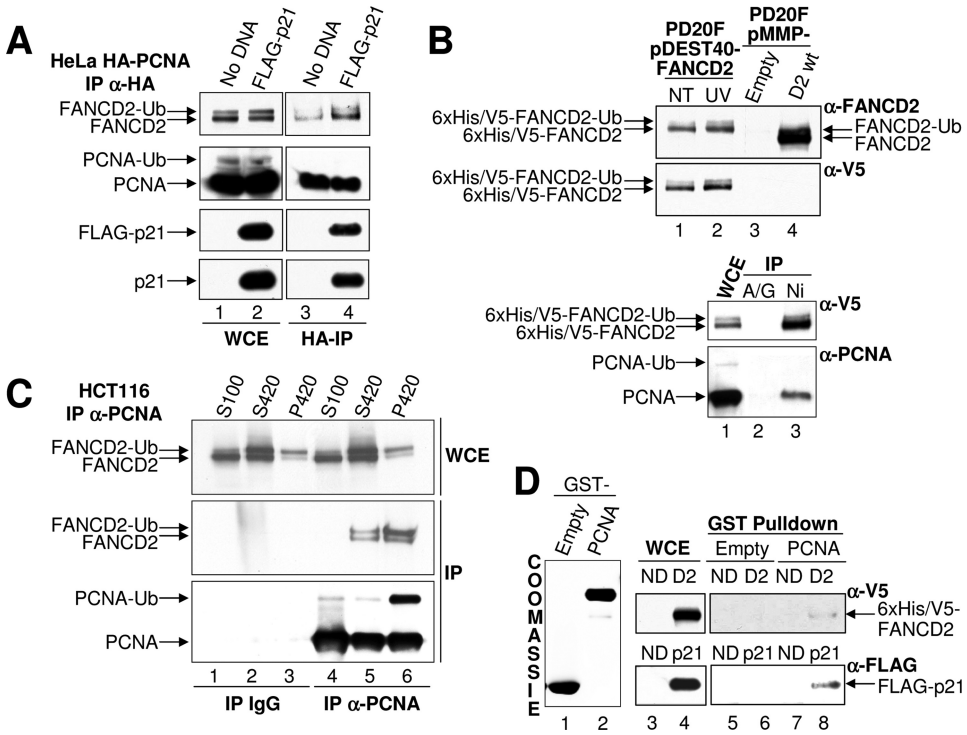

FIGURE 1. **Co-immunoprecipitation of FANCD2 and PCNA.** *A*, HeLa cells stably expressing HA-PCNA were untransfected or transiently transfected with the mammalian expression vector pMT5-FLAG-p21. HA-PCNA immune complexes were immunoprecipitated with anti-HA agarose, resolved, and immunoblotted with anti-FANCD2, -PCNA, -FLAG, and -p21 antibodies. *B*, PD20F pDEST40-FANCD2 cells, stably expressing 6xHis/V5-FANCD2, were treated with 20 J/m^2 UV irradiation and WCE prepared 4 h later. WCE were resolved and immunoblotted with anti-FANCD2 and anti-V5 antibodies. For the Ni^{2+} pull-down, WCE from PD20F pDEST40-FANCD2 cells were incubated with protein A/G-agarose or Ni^{2+} beads for 1 h at 4 °C, and bound proteins were immunoblotted with anti-PCNA and anti-V5 antibodies. *C*, HCT116 cells were treated with 40 J/m^2 UV irradiation and 4 h later lysed in NETN lysis buffer containing 100 mM or 420 mM NaCl without and with sonication to yield S100, S420, and P420 fractions, respectively. Lysates were incubated with anti-PCNA antibody or control mouse IgG. Immunoprecipitates were analyzed by immunoblotting with anti-FANCD2 and anti-PCNA antibodies. *D*, COS-7 cells were transiently transfected with the mammalian expression vectors pDEST40-FANCD2 or pMT5-FLAG-p21 and WCE incubated with GST-Empty and GST-PCNA recombinant proteins. Bound proteins were resolved and immunoblotted with anti-V5 and anti-FLAG antibodies. *IP*, immunoprecipitation. *PD*, pull-down. *ND*, no DNA.

PCNA from chromatin fractions prepared from untreated and UV-irradiated HCT116 cells (supplemental Fig. S1, *lower panel*, *lanes 3* and *4*). In support of a direct interaction between FANCD2 and PCNA, GST-PCNA, and not GST alone, bound to 6xHis/V5-FANCD2 overexpressed in COS-7 cells (Fig. 1*D*, *lanes 6* and *8*). For this experiment, COS-7 cells overexpressing FLAG-p21 was used as a positive control (Fig. 1*D*, *lane 8*).

FANCD2 Contains a Highly Conserved Putative PCNA Interaction Motif—We identified two putative PIP-box motifs in FANCD2: one at amino acids 527–534 and a second at amino acids 1063–1070. The PIP-box at amino acids 527–534 demonstrated high conservation and was selected for further analysis. The four essential FANCD2 PIP$^{527-534}$-box amino acids were mutated to alanines (Fig. 2*A*), and the pMMP-FANCD2 PIPΔ retroviral vector generated. PD20F (FA-D2) patient cells were transduced with pMMP-FANCD2 PIPΔ, to generate the PD20F pMMP-FANCD2 PIPΔ cell line. To analyze the effect of mutation of the FANCD2 PIP-box on the FANCD2-PCNA interaction, PCNA immune complexes were immunoprecipitated from PD20F pMMP-Empty, -FANCD2 wt, -FANCD2 K561R (that cannot be mono-ubiquitinated) (3), and -FANCD2 PIPΔ cells, and immunoblotted with anti-FANCD2. As expected, FANCD2 wt readily co-immunoprecipitated with PCNA (Fig. 2*B*). FANCD2 K561R also co-immunoprecipitated with PCNA, albeit less efficiently (~3-fold reduction) than FANCD2 wt (Fig. 2*B* and supplemental Fig. S2*A*). Finally, negligible levels of FANCD2 PIPΔ co- immunoprecipitated with PCNA (Fig. 2*B* and supplemental Fig. S2*A*). Immunoblotting with a rabbit polyclonal anti-PCNA antibody confirmed the presence of equal amounts of PCNA immune complexes in all four cell lines (Fig. 2*B*).

Next, COS-7 cells were transiently transfected with 6xHis/V5-FANCD2 wt, -FANCD2 K561R, and -FANCD2 PIPΔ mammalian expression constructs. Similar to that observed above, 6xHis/V5-FANCD2 wt co-immunoprecipitated with PCNA (Fig. 2*C*). 6xHis/V5-FANCD2 K561R also co-immunoprecipitated with PCNA, although again less efficiently than 6xHis/V5-FANCD2 wt (Fig. 2*C* and supplemental Fig. S2*B*). Finally, negligible levels of 6xHis/V5-FANCD2 PIPΔ co-immunoprecipitated with PCNA (Fig. 2*C*). When corrected for total 6xHis/V5-FANCD2 PIPΔ protein levels, this corresponded to an approximate 9-fold reduction in association between PCNA and 6xHis/V5-FANCD2 PIPΔ, compared with 6xHis/V5-FANCD2 wt (supplemental Fig. S2*B*).

The FANCE protein has been proposed to form a molecular bridge between the core FA complex and FANCD2, and has been demonstrated to bind directly to FANCD2 (28). To analyze the effect of mutation of the FANCD2 PIP-box on the FANCD2-FANCE interaction, we transiently transfected PD20F pMMP-Empty, -FANCD2 wt, -FANCD2 K561R, and -FANCD2 PIPΔ cells with a FLAG-tagged FANCE construct, and examined the association between FANCD2 and FLAG-FANCE (Fig. 2*D*). The use of an epitope-tagged FANCE construct was required for this experiment because of the absence of a suitable commercially available FANCE antibody. When normalized for total FANCD2 protein levels, approximately equal amounts of FANCD2 wt, FANCD2 K561R, and FANCD2 PIPΔ co-immunoprecipitated with FLAG-FANCE, indicating that the FANCD2 PIPΔ mutant protein retains the ability to associate with FANCE (Fig. 2*D* and supplemental Fig. S2*C*). We also sought to determine if mutation of the FANCD2 PIP-box disrupted the interaction between FANCD2 and FANCI. However, we were unable to co-immunoprecipitate FANCD2 wt and FANCI, precluding us from addressing this question. Collectively, these results suggest that the interaction between

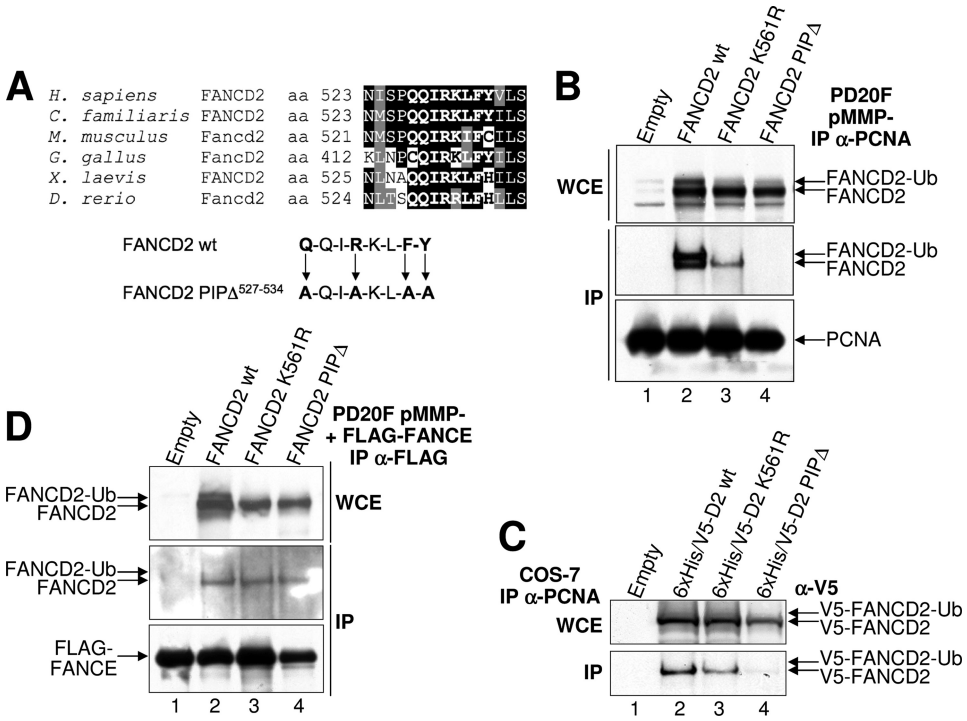

FIGURE 2. **The FANCD2 PIP-box motif is required for the FANCD2-PCNA interaction.** *A*, BLAST alignment of FANCD2 homologues demonstrating conservation of the human FANCD2 PIP-box, and mutation strategy. *B*, decreased association of the FANCD2 PIPΔ mutant with PCNA. WCE were incubated with anti-PCNA antibody, and immune complexes were resolved and immunoblotted with anti-FANCD2 and anti-PCNA antibodies. *C*, COS-7 cells were transiently transfected with the indicated pDEST40-FANCD2 constructs. 48 h later, WCE were prepared, incubated with anti-PCNA antibody, and immune complexes were resolved and immunoblotted with anti-V5 antibody. *D*, association of the FANCD2 PIPΔ mutant protein with FANCE. Cells were transiently transfected with the pEAK8-FLAG-FANCE construct (28) and 48 h later WCE incubated with anti-FLAG antibody. Immune complexes were resolved and immunoblotted with anti-FANCD2 and anti-FLAG antibodies. *IP*, immunoprecipitation.

FANCD2 and PCNA is mediated by a putative FANCD2 PIP-box that is dispensable for FANCD2-FANCE binding.

Mutation of the FANCD2 PIP-box Motif Abrogates FANCD2 Mono-ubiquitination—Next, we examined the effects of mutation of the FANCD2 PIP-box on FANCD2 mono-ubiquitination. PD20F pMMP-Empty, -FANCD2 wt, -FANCD2 K561R, and -FANCD2 PIPΔ cells were exposed to 1.0 μM APH for 24 h, 60 J/m^2 UV irradiation, or 15 Gy X-irradiation. Strong induction of wt FANCD2 mono-ubiquitination was observed for all treatments. For example, exposure to 1.0 μM APH for 24 h increased the FANCD2-Ub:FANCD2 ratio ~2-fold (Fig. 3*A*). However, like FANCD2 K561R, the FANCD2 PIP-box mutant protein failed to undergo both spontaneous or DNA damage-inducible mono-ubiquitination (Fig. 3, *A–C*). Conversely, UV-inducible PCNA mono-ubiquitination was observed for all cell lines (Fig. 3*B*).

We next examined the ability of the FANCD2 PIP-box mutant to undergo UV-inducible, ATR-mediated phosphorylation (13, 29). Whole-cell lysates prepared from untreated and UV-irradiated PD20F pMMP-FANCD2 wt and -FANCD2 PIPΔ cells were incubated in the absence or presence of λ phosphatase. As expected, λ phosphatase treatment accelerated the migration of FANCD2 wt (Fig. 3*D*, *lanes 1–4*). Similarly, λ phosphatase treatment accelerated the migration of both untreated and UV-irradiated FANCD2 PIPΔ (Fig. 3*D*, *lanes 5–8*). Collectively, these results indicate that the FANCD2 PIP-box mutant fails to undergo both spontaneous and DNA damage-inducible mono-ubiquitination, yet remains competent for ATR-mediated phosphorylation.

The FANCD2 PIP-box Mutant Localizes to Chromatin Yet Fails to Form Nuclear Foci—We next examined the subcellular localization of the FANCD2 PIPΔ mutant protein. Cells were lysed in a hypotonic buffer to extract cytoplasmic proteins (S1). The remaining pellets were lysed in a high-salt buffer to extract soluble nuclear proteins (S2). Salt-extracted pellets were subsequently treated with micrococcal nuclease to release chromatin-associated proteins, characterized by the presence of the nucleosomal histone H2A (S3) (30). We detected mono-ubiquitinated FANCD2 in the S2 and S3 fractions, in the absence and presence of MMC, as expected (Fig. 4*A*, *upper panel*, *lanes 9–12*). However, we also detected both non-ubiquitinated FANCD2 K561R and FANCD2 PIPΔ in all three fractions, in the absence and presence of MMC (Fig. 4*A*), indicating that the FANCD2 PIPΔ mutant protein remains competent for chromatin localization. A similar observation has previously been described for FANCD2 K561R (31).

We next examined the ability of the FANCD2 PIP-box mutant protein to assemble into discrete nuclear foci. Following exposure to APH, FANCD2 wt formed discrete nuclear foci as previously reported (3, 4) (Fig. 4*B*). However, like FANCD2 K561R (3), FANCD2 PIPΔ failed to form nuclear foci in the absence or presence of APH. Instead, we consistently observed non-punctate staining patterns, including diffuse nuclear as well as concentrated nucleolar staining (Fig. 4*B*).

FANCD2 Mono-ubiquitination Promotes Its Stabilization in Chromatin—We next determined the protein half-lives of FANCD2-Ub, FANCD2 wt, FANCD2 K561R, and FANCD2 PIPΔ. Cells were exposed to the translation inhibitor cycloheximide and protein levels monitored over a 24 h period. FANCD2 K561R and FANCD2 PIPΔ exhibited significantly shorter half-lives than both FANCD2-Ub and FANCD2 wt. For example, 3 h following exposure to cycloheximide FANCD2 wt, K561R, and PIPΔ protein levels had decreased by ~23, 38, and 81%, respectively (Fig. 5, *A* and *B*). In contrast, wild-type FANCD2-Ub protein levels increased ~28%, and remained elevated 24 h following the addition of cycloheximide. These results indicate that the mono-ubiquitination of FANCD2 promotes its stabilization in chromatin, and

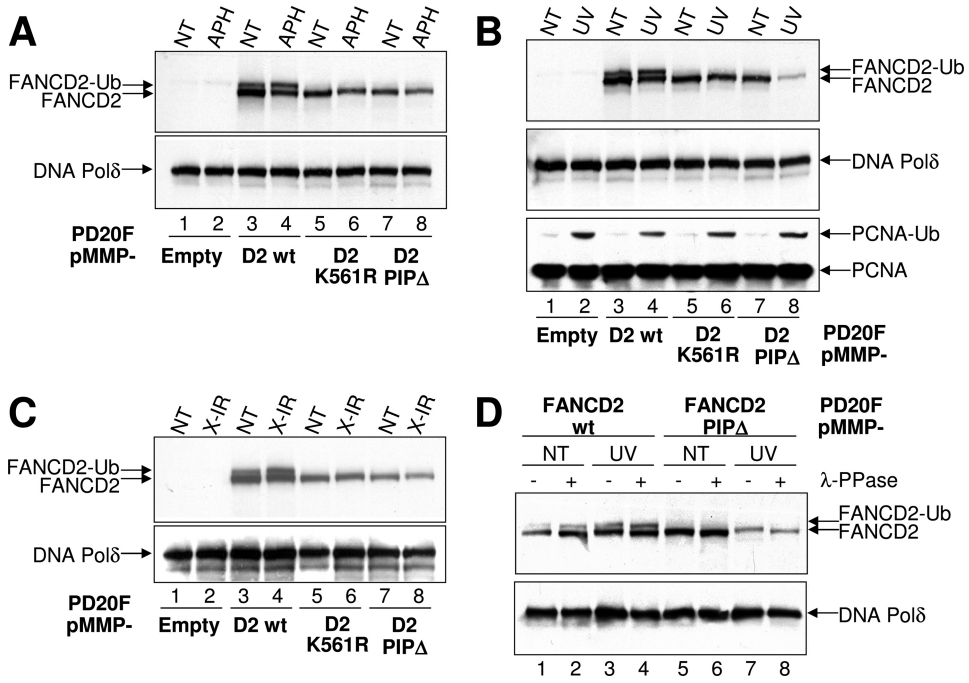

FIGURE 3. **The FANCD2 PIP-box motif is required for both spontaneous and DNA damage-inducible FANCD2 mono-ubiquitination.** *A*, cells were untreated (*NT*) or exposed to 1.0 μM APH for 24 h (*APH*), and WCE were immunoblotted with the indicated antibodies. The catalytic subunit of DNA Pol δ was used as a protein loading control. *B*, cells were untreated (*NT*) or exposed to 60 J/m^2 UV irradiation (*UV*), and 4 h later whole-cell lysates were prepared and immunoblotted with the indicated antibodies. *C*, cells were untreated (*NT*) or exposed to 15 Gy X-irradiation (*X-IR*). Whole-cell lysates were prepared 3 h post-irradiation and immunoblotted with the indicated antibodies. *D*, PD20F pMMP-FANCD2 wt and -FANCD2 PIPΔ were untreated (*NT*) or exposed to 60 J/m^2 UV irradiation (*UV*), and 4 h later, whole-cell lysates were prepared and incubated in the presence or absence of λ phosphatase (λ-*P Pase*), prior to immunoblotting with the indicated antibodies.

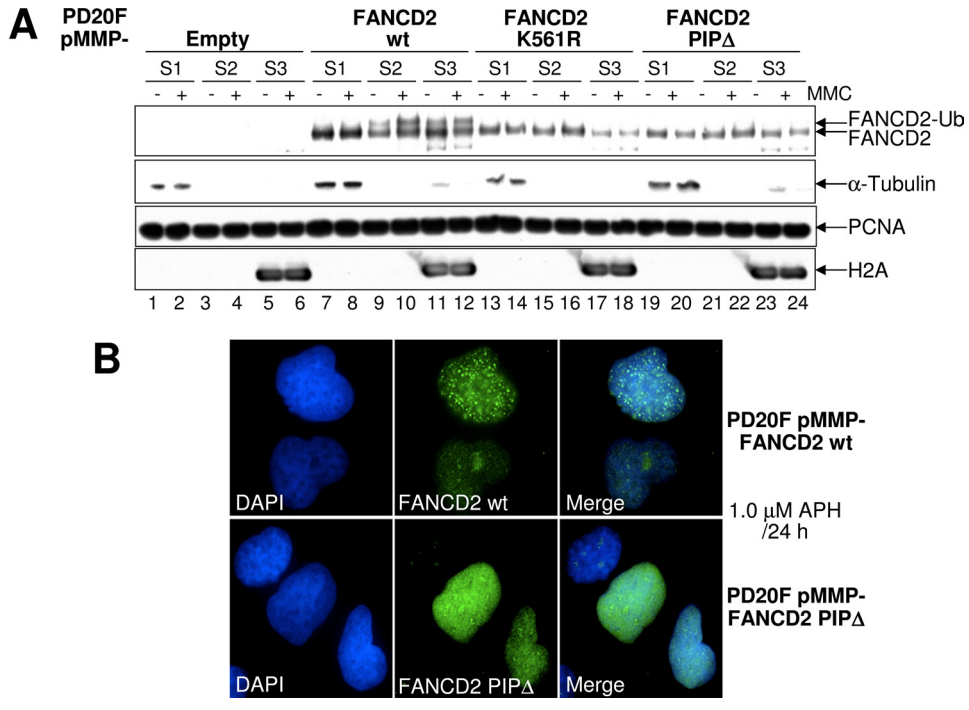

FIGURE 4. **The FANCD2 PIP-box mutant localizes to chromatin yet fails to assemble into nuclear foci.** *A*, cells were incubated in the absence and presence of 120 nM MMC for 18 h, fractionated into cytoplasmic (*S1*), soluble nuclear (*S2*), and chromatin-associated fractions (*S3*), and immunoblotted with antibodies to FANCD2, α-tubulin, PCNA, and H2A. *B*, FANCD2 PIP-box mutant fails to assemble into nuclear foci. PD20F pMMP-FANCD2 wt and pMMP-FANCD2 PIPΔ cells were incubated in the absence or presence of 1.0 μM APH for 24 h, fixed, and stained with rabbit polyclonal anti-FANCD2 E35 (*green*) antibody, and counterstained with 4′,6-diamidino-2-phenylindole (DAPI) (*blue*).

that mutation of Lys-561 and the PIP-box significantly reduces the protein half-life.

The FANCD2 PIP-box Motif Mutant Fails to Correct the Cellular Phenotypes of FA-D2 Patient Cells—We next determined if the FANCD2 PIPΔ mutant could rescue the MMC hypersensitivity of PD20F cells. In contrast to FANCD2 wt, the FANCD2 PIPΔ mutant failed to rescue the MMC sensitivity of PD20F cells. For example, at 60 nM MMC, a 2.4-fold increase in sensitivity ($p < 0.05$) to the lethal effects of MMC was observed for PD20F pMMP-FANCD2 PIPΔ cells compared with PD20F pMMP-FANCD2 wt cells (Fig. 6*A*). We also measured the frequency of chromosome gaps, breaks, and radial formations in metaphase spreads prepared from cells treated with APH or MMC. As expected, exposure to APH and MMC induced significantly elevated levels of chromosome aberrations in PD20F pMMP-Empty cells, 6.2-fold ($p < 0.0001$) and 2.1-fold ($p = 0.0093$), respectively, compared with untreated cells (Fig. 6*B*). Expression of FANCD2 wt corrected the elevated APH- ($p = 0.0315$) and MMC- ($p = 0.001$) induced chromosome aberrations of PD20F cells. However, expression of either FANCD2 K561R or FANCD2 PIPΔ failed to correct the elevated frequency of APH- and MMC-induced chromosome aberrations. Like PD20F pMMP-Empty, a 6.0-fold ($p < 0.0001$) and 2.4-fold ($p = 0.0026$) increase in chromosome aberrations was observed for PD20F pMMP-FANCD2 PIPΔ cells following treatment with APH and MMC, respectively, compared with untreated cells (Fig. 6*B*). Finally, using flow cytometry, we examined cell cycle progression in the absence or presence of MMC. Like PD20F pMMP-Empty and -FANCD2 K561R cells, PD20F pMMP-FANCD2 PIPΔ cells displayed a prolonged accumulation in G2 phase of the cell cycle following exposure to MMC. For example, a ~2-fold greater proportion of PD20F pMMP-FANCD2 PIPΔ cells

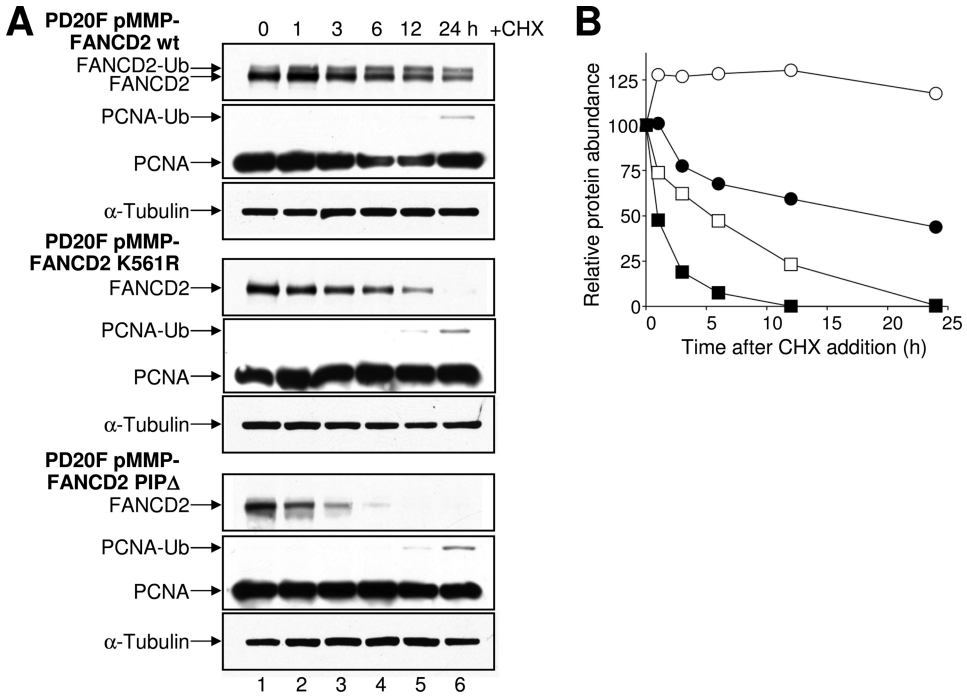

FIGURE 5. **The mono-ubiquitination of FANCD2 promotes its chromatin stabilization.** *A*, cells were treated with cycloheximide (*CHX*) and whole-cell lysates immunoblotted with antibodies against FANCD2, PCNA, and α-tubulin. *B*, FANCD2 protein band intensities from Fig. 6*A* were quantified using ImageJ and plotted. FANCD2-Ub (○), FANCD2 wt (non-ubiquitinated) (●), FANCD2 K561R (□), FANCD2 PIPΔ (■).

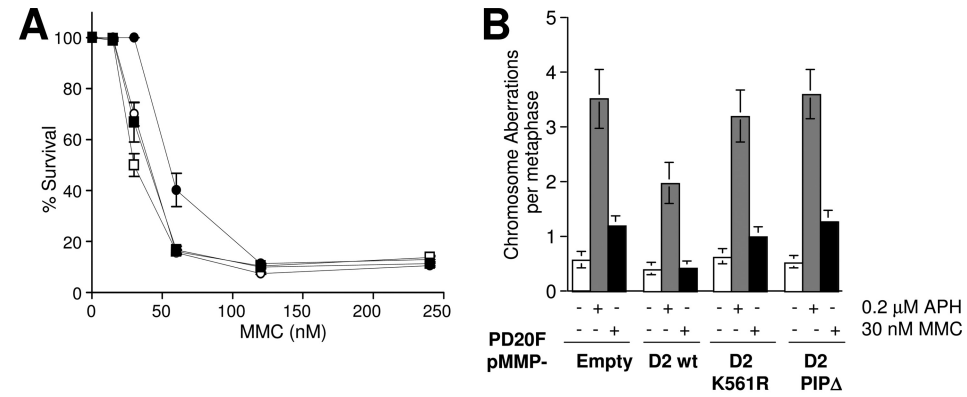

	PD20F -Empty		-FANCD2 wt		-FANCD2 K561R		-FANCD2 PIPΔ	
	NT	MMC	NT	MMC	NT	MMC	NT	MMC
G1 (%)	39.6	16.2	36.7	23.8	40.9	16.0	47.3	16.3
S (%)	48.0	36.9	49.9	44.3	44.0	34.0	34.9	27.5
G2/M (%)	12.4	46.9	13.5	32.9	15.1	50.0	17.8	56.2

FIGURE 6. **The FANCD2 PIP-box mutant fails to rescue the cellular phenotypes of PD20F (FA-D2) cells.** *A*, PD20F (FA-D2) pMMP-Empty (○), -FANCD2 wt (●), -FANCD2 K561R (□), and -FANCD2 PIPΔ (■) were treated with MMC for 10–14 days. *Error bars* represent the S.E. from triplicate measurements, and are smaller than the dimensions of the symbols for several points. This experiment was performed three times with similar findings. *B*, same cells were untreated (*white bars*) or exposed to 0.2 μM APH (*gray bars*) or 30 nM MMC (*black bars*) for 24 h, and chromosome aberrations quantified. At least 30 metaphases were scored for each treatment. *Error bars* indicate the S.E. This experiment was performed three times with similar findings. *C*, for the G2 accumulation assay cells were untreated (*NT*) or exposed to 75 nM MMC for 48 h, fixed, stained with propidium iodide, and analyzed by flow cytometry.

accumulated in G2/M following exposure to MMC, compared with PD20F pMMP-FANCD2 wt cells (Fig. 6*C*). Collectively these results strongly suggest that the FANCD2 PIP-box is essential for the function of FANCD2 in the cellular DNA damage response.

DISCUSSION

In support of an important role for the FA-BRCA pathway in a S-phase DNA repair process, both spontaneous and DNA crosslink-induced FANCD2 mono-ubiquitination and nuclear foci formation occur almost exclusively during S-phase (9, 32, 33). Thus, it is likely that a stalled or collapsed DNA replication fork is a major stimulus for the mono-ubiquitination of FANCD2. The mechanism by which FANCD2 is recruited to damaged DNA replication forks has not, however, been determined. Here, we describe an important interaction between the FANCD2 and PCNA proteins. We demonstrate that FANCD2 and PCNA associate in chromatin, and that this association is dependent on a highly conserved FANCD2 PIP-box motif. Furthermore, disruption of this motif abrogates both spontaneous and DNA damage-inducible FANCD2 mono-ubiquitination. Our results suggest that the association between PCNA and FANCD2 may be an important prerequisite for the mono-ubiquitination of FANCD2 and, consequently, its DNA repair function. A similar auxiliary role for PCNA, also mediated *via* PIP-box interactions, has been established for several DNA repair enzymes including MSH3, XPG, and XPV/Pol η (34–37). The association of FANCD2 with PCNA in a DNA damage surveillance capacity represents an attractive model for the localization of FANCD2 to sites of DNA damage encountered by the DNA replisome.

That the mutation of the FANCD2 PIP-box completely abrogated both spontaneous and DNA damage-inducible FANCD2 mono-ubiquitination was unexpected. To our knowledge, only one other FANCD2 mutation, that of the site of ubiquitin conjugation itself, Lys-561, has been described that leads to a complete loss of FANCD2 mono-ubiquitination (3). We could not rule out the possibility that a change in protein

folding underlies the inability of the FANCD2 PIP-box mutant to undergo mono-ubiquitination, as the PIP-box is proximal to Lys-561 (3). Thus, a localized alteration in protein folding may preclude access of the FA E2/E3 holoenzyme to Lys-561. Several lines of evidence, however, argue against a gross structural alteration. First, like FANCD2 wt, the FANCD2 PIPΔ mutant retained the ability to interact with FANCE, a core FA complex protein previously demonstrated to bind directly to FANCD2 (28). Second, the FANCD2 PIPΔ mutant protein underwent DNA damage-inducible phosphorylation (13, 29). Third, the FANCD2 PIPΔ mutant protein localized to chromatin. These results suggest that the mutant protein retains structural integrity and at least partial functionality. Nevertheless, we cannot rule out the possibility of a localized effect, or that mutation of the PIP-box precludes the interaction of FANCD2 with a protein, other than PCNA, required for its efficient mono-ubiquitination.

The mono-ubiquitination of FANCD2 has previously been hypothesized to be required for its targeting to chromatin (27). However, in this study, albeit using a different subcellular fractionation protocol, we detected non-ubiquitinated FANCD2 K561R and FANCD2 PIPΔ proteins in chromatin. We propose that mono-ubiquitination stabilizes FANCD2 in chromatin, and that non-ubiquitinated FANCD2 fails to be retained in chromatin. In support of a chromatin-dependent FANCD2 mono-ubiquitination model, the FANCD2 E2 ubiquitin-conjugating enzyme UBE2T (38) has been demonstrated to be constitutively chromatin-localized, independent of DNA damage or cell cycle stage (31). Furthermore, the FA core complex localizes to chromatin, and its E3 ubiquitin ligase activity is dependent on its DNA damage-induced chromatin localization (31, 39). Thus, we hypothesize that the association between FANCD2 and PCNA may facilitate the FA E2/E3 holoenzyme-mediated mono-ubiquitination of FANCD2, and its stabilization and retention in chromatin until USP1-mediated de-ubiquitination and chromatin release (40). Consistent with this, we have also demonstrated that mono-ubiquitinated FANCD2 displays a longer protein half-life than FANCD2 K561R and, in particular, FANCD2 PIPΔ. Mono-ubiquitin may serve as a molecular adaptor between PCNA-associated FANCD2 and an as yet unidentified ubiquitin-binding domain (UBD)-containing chromatin-associated protein. In support of this hypothesis, Matsushita *et al.* (41) demonstrated that a chicken DT40 FANCD2-Ub chimeric protein harboring an I44A mutation in the essential hydrophobic patch of ubiquitin (that disrupts ubiquitin-UBD binding) could only weakly complement the cisplatin sensitivity of *fancd2* cells. Several candidate chromatin-associated ubiquitin receptors exist, including XPV/Pol η, REV1, or one of the core FA complex proteins.

An important FANCD2 mono-ubiquitination-independent function for the FA core complex in REV1-mediated TLS has been demonstrated (11): FANCA and FANCG, yet not FANCD2, were demonstrated to be required for the efficient assembly of the REV1 protein into nuclear foci (11). It has recently been proposed that the mono-ubiquitination of PCNA may be required for a post-replicative DNA repair process, for example daughter-strand gap (DSG) repair (12, 42, 43). As DSG repair is thought to involve both TLS and a HR-mediated template switching process (12, 43), we propose a model whereby FANCD2 and PCNA, through a mono-ubiquitination-dependent process, may function in the HR repair of DSGs (Fig. 7). This is consistent with several studies indicating a role for the FA proteins in an undefined HR process, as well as earlier observations that the major HR proteins BRCA1, FANCD1/BRCA2, and RAD51, co-localize with PCNA and FANCD2 in nuclear foci during S-phase (44, 45).

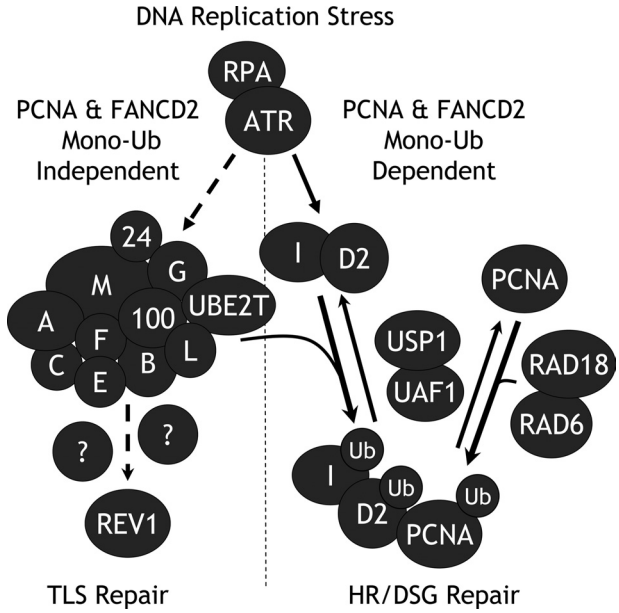

FIGURE 7. **A speculative model depicting mono-ubiquitination-dependent and independent functions of the FA-BRCA pathway in DNA replication-associated repair processes.** In response to DNA damage encountered by the DNA replisome, the FA core complex (*a*) promotes the formation of REV1 nuclear foci in a rapid error-prone TLS pathway (11) and (*b*) promotes the mono-ubiquitination of FANCD2 and FANCI, which, together with mono-ubiquitinated PCNA (42), may promote a post-replicative, HR-dependent DSG repair mechanism.

In summary, our findings strongly suggest that the FANCD2 protein associates with PCNA in a DNA damage surveillance capacity via a highly conserved PIP-box. Upon encounter of a lesion-damaged template during DNA replication, PCNA-associated FANCD2 becomes mono-ubiquitinated *via* the concerted activity of the core FA complex, the FANCL ubiquitin ligase, and the UBE2T E2 ubiquitin-conjugating enzyme, thus facilitating its function in DNA repair. The erroneous or untimely repair of damaged DNA replication forks could lead to the generation of the complex, unbalanced chromosomal abnormalities frequently observed in FA cancer cells. Our findings have significant implications for our understanding of the DNA damage surveillance and repair mechanisms activated upon DNA replication fork arrest, and lend further insight into the molecular etiology of a rare, yet highly important, cancer susceptibility syndrome.

Acknowledgments—We thank members of the Howlett and Glover laboratories, Paul R. Andreassen, Martin F. Arlt, Alan D. D'Andrea, Caixia Guo, and John V. Moran for helpful discussions. We thank K. J. Patel for the FANCE-2×Flag construct.

REFERENCES

1. Taniguchi, T., and D'Andrea, A. D. (2006) *Blood* **107,** 4223–4233
2. *Fanconi Anemia: Standards for Clinical Care*, 2nd Ed., Fanconi Anemia Research Fund, Inc., Eugene, OR
3. Garcia-Higuera, I., Taniguchi, T., Ganesan, S., Meyn, M. S., Timmers, C., Hejna, J., Grompe, M., and D'Andrea, A. D. (2001) *Mol. Cell.* **7,** 249–262
4. Howlett, N. G., Taniguchi, T., Durkin, S. G., D'Andrea, A. D., and Glover, T. W. (2005) *Hum. Mol. Genet.* **14,** 693–701
5. Wang, W. (2007) *Nat. Rev. Genet.* **8,** 735–748
6. Rego, M. A., Kolling, F. W., 4th, and Howlett, N. G. (2009) *Mutat. Res.* **668,** 27–41
7. Hussain, S., Wilson, J. B., Medhurst, A. L., Hejna, J., Witt, E., Ananth, S., Davies, A., Masson, J. Y., Moses, R., West, S. C., De Winter, J. P., Ashworth, A., Jones, N. J., and Mathew, C. G. (2004) *Hum. Mol. Genet.* **13,** 1241–1248
8. Smogorzewska, A., Matsuoka, S., Vinciguerra, P., McDonald, E. R., 3rd, Hurov, K. E., Luo, J., Ballif, B. A., Gygi, S. P., Hofmann, K., D'Andrea, A. D., and Elledge, S. J. (2007) *Cell.* **129,** 289–301
9. Taniguchi, T., Garcia-Higuera, I., Andreassen, P. R., Gregory, R. C., Grompe, M., and D'Andrea, A. D. (2002) *Blood* **100,** 2414–2420
10. Howlett, N. G., Taniguchi, T., Olson, S., Cox, B., Waisfisz, Q., De Die-Smulders, C., Persky, N., Grompe, M., Joenje, H., Pals, G., Ikeda, H., Fox, E. A., and D'Andrea, A. D. (2002) *Science* **297,** 606–609
11. Mirchandani, K. D., McCaffrey, R. M., and D'Andrea, A. D. (2008) *DNA Repair* **7,** 902–911
12. Niedzwiedz, W., Mosedale, G., Johnson, M., Ong, C. Y., Pace, P., and Patel, K. J. (2004) *Mol. Cell.* **15,** 607–620
13. Andreassen, P. R., D'Andrea, A. D., and Taniguchi, T. (2004) *Genes Dev.* **18,** 1958–1963
14. Collis, S. J., Barber, L. J., Clark, A. J., Martin, J. S., Ward, J. D., and Boulton, S. J. (2007) *Nat. Cell Biol.* **9,** 391–401
15. Wang, X., Kennedy, R. D., Ray, K., Stuckert, P., Ellenberger, T., and D'Andrea, A. D. (2007) *Mol. Cell. Biol.* **27,** 3098–3108
16. Hoege, C., Pfander, B., Moldovan, G. L., Pyrowolakis, G., and Jentsch, S. (2002) *Nature.* **419,** 135–141
17. Kannouche, P. L., Wing, J., and Lehmann, A. R. (2004) *Mol. Cell.* **14,** 491–500
18. Meetei, A. R., de Winter, J. P., Medhurst, A. L., Wallisch, M., Waisfisz, Q., van de Vrugt, H. J., Oostra, A. B., Yan, Z., Ling, C., Bishop, C. E., Hoatlin, M. E., Joenje, H., and Wang, W. (2003) *Nat. Genet.* **35,** 165–170
19. Watanabe, K., Tateishi, S., Kawasuji, M., Tsurimoto, T., Inoue, H., and Yamaizumi, M. (2004) *EMBO J.* **23,** 3886–3896
20. Huang, T. T., Nijman, S. M., Mirchandani, K. D., Galardy, P. J., Cohn, M. A., Haas, W., Gygi, S. P., Ploegh, H. L., Bernards, R., and D'Andrea, A. D. (2006) *Nat. Cell Biol.* **8,** 339–347
21. Nijman, S. M., Huang, T. T., Dirac, A. M., Brummelkamp, T. R., Kerkhoven, R. M., D'Andrea, A. D., and Bernards, R. (2005) *Mol. Cell.* **17,** 331–339
22. Moldovan, G. L., Pfander, B., and Jentsch, S. (2007) *Cell.* **129,** 665–679
23. Warbrick, E. (1998) *Bioessays.* **20,** 195–199
24. Xia, B., Sheng, Q., Nakanishi, K., Ohashi, A., Wu, J., Christ, N., Liu, X., Jasin, M., Couch, F. J., and Livingston, D. M. (2006) *Mol. Cell.* **22,** 719–729
25. Guo, C., Sonoda, E., Tang, T. S., Parker, J. L., Bielen, A. B., Takeda, S., Ulrich, H. D., and Friedberg, E. C. (2006) *Mol. Cell.* **23,** 265–271
26. Näf, D., Kupfer, G. M., Suliman, A., Lambert, K., and D'Andrea, A. D. (1998) *Mol. Cell. Biol.* **18,** 5952–5960
27. Montes de Oca, R., Andreassen, P. R., Margossian, S. P., Gregory, R. C., Taniguchi, T., Wang, X., Houghtaling, S., Grompe, M., and D'Andrea, A. D. (2005) *Blood* **105,** 1003–1009
28. Pace, P., Johnson, M., Tan, W. M., Mosedale, G., Sng, C., Hoatlin, M., de Winter, J., Joenje, H., Gergely, F., and Patel, K. J. (2002) *EMBO J.* **21,** 3414–3423
29. Ho, G. P., Margossian, S., Taniguchi, T., and D'Andrea, A. D. (2006) *Mol. Cell. Biol.* **26,** 7005–7015
30. Mosedale, G., Niedzwiedz, W., Alpi, A., Perrina, F., Pereira-Leal, J. B., Johnson, M., Langevin, F., Pace, P., and Patel, K. J. (2005) *Nat. Struct. Mol. Biol.* **12,** 763–771
31. Alpi, A., Langevin, F., Mosedale, G., Machida, Y. J., Dutta, A., and Patel, K. J. (2007) *Mol. Cell. Biol.* **27,** 8421–8430
32. Akkari, Y. M., Bateman, R. L., Reifsteck, C. A., Olson, S. B., and Grompe, M. (2000) *Mol. Cell. Biol.* **20,** 8283–8289
33. Rothfuss, A., and Grompe, M. (2004) *Mol. Cell. Biol.* **24,** 123–134
34. Acharya, N., Yoon, J. H., Gali, H., Unk, I., Haracska, L., Johnson, R. E., Hurwitz, J., Prakash, L., and Prakash, S. (2008) *Proc. Natl. Acad. Sci. U.S.A.* **105,** 17724–17729
35. Gary, R., Ludwig, D. L., Cornelius, H. L., MacInnes, M. A., and Park, M. S. (1997) *J. Biol. Chem.* **272,** 24522–24529
36. Haracska, L., Johnson, R. E., Unk, I., Phillips, B., Hurwitz, J., Prakash, L., and Prakash, S. (2001) *Mol. Cell. Biol.* **21,** 7199–7206
37. Kleczkowska, H. E., Marra, G., Lettieri, T., and Jiricny, J. (2001) *Genes Dev.* **15,** 724–736
38. Machida, Y. J., Machida, Y., Chen, Y., Gurtan, A. M., Kupfer, G. M., D'Andrea, A. D., and Dutta, A. (2006) *Mol. Cell.* **23,** 589–596
39. Mi, J., and Kupfer, G. M. (2005) *Blood* **105,** 759–766
40. Oestergaard, V. H., Langevin, F., Kuiken, H. J., Pace, P., Niedzwiedz, W., Simpson, L. J., Ohzeki, M., Takata, M., Sale, J. E., and Patel, K. J. (2007) *Mol. Cell.* **28,** 798–809
41. Matsushita, N., Kitao, H., Ishiai, M., Nagashima, N., Hirano, S., Okawa, K., Ohta, T., Yu, D. S., McHugh, P. J., Hickson, I. D., Venkitaraman, A. R., Kurumizaka, H., and Takata, M. (2005) *Mol. Cell.* **19,** 841–847
42. Edmunds, C. E., Simpson, L. J., and Sale, J. E. (2008) *Mol. Cell.* **30,** 519–529
43. Nagaraju, G., and Scully, R. (2007) *DNA Repair* **6,** 1018–1031
44. Chen, J., Silver, D. P., Walpita, D., Cantor, S. B., Gazdar, A. F., Tomlinson, G., Couch, F. J., Weber, B. L., Ashley, T., Livingston, D. M., and Scully, R. (1998) *Mol. Cell.* **2,** 317–328
45. Scully, R., Chen, J., Ochs, R. L., Keegan, K., Hoekstra, M., Feunteun, J., and Livingston, D. M. (1997) *Cell* **90,** 425–435

Functional Interaction between the Fanconi Anemia D2 Protein and Proliferating Cell Nuclear Antigen (PCNA) via a Conserved Putative PCNA Interaction Motif

Niall G. Howlett, Julie A. Harney, Meghan A. Rego, Frederick W. Kolling IV and Thomas W. Glover

J. Biol. Chem. 2009, 284:28935-28942.
doi: 10.1074/jbc.M109.016352 originally published online August 24, 2009

SUPPLEMENTAL FIGURE LEGENDS

FIGURE S1. Co-immunoprecipitation of FANCD2 and PCNA in chromatin. HCT116 cells were untreated (NT) or exposed to 40 J/m^2 UV irradiation (UV) and allowed to recover for 4 h prior to triton extraction and crosslinking as described (17). Triton-soluble (S100) and triton-insoluble (P300) proteins were incubated with a rabbit polyclonal antibody against FANCD2 or rabbit serum. Immune complexes were resolved and immunoblotted with mouse monoclonal antibodies against FANCD2 and PCNA.

FIGURE S2. Bar charts depicting the quantification of protein band intensities from Figure 2. *A*, Quantification of protein band intensities from Figure 2B, demonstrating the decreased association between PCNA and the FANCD2 PIPΔ mutant. *B*, Quantification of protein band intensities from Figure 2C, demonstrating the decreased association between PCNA and the 6xHis/V5-FANCD2 PIPΔ mutant. *C*, Quantification of protein band intensities from Figure 2D, demonstrating approximately equal levels of association between FLAG-FANCE and FANCD2 wt, FANCD2 K561R, and FANCD2 PIPΔ. The white bars represent values from the input bands (W) while the black bars represent values from the immunprecipitation bands (IP). Protein band intensities were quantified using Scion Image.

FIGURE S1

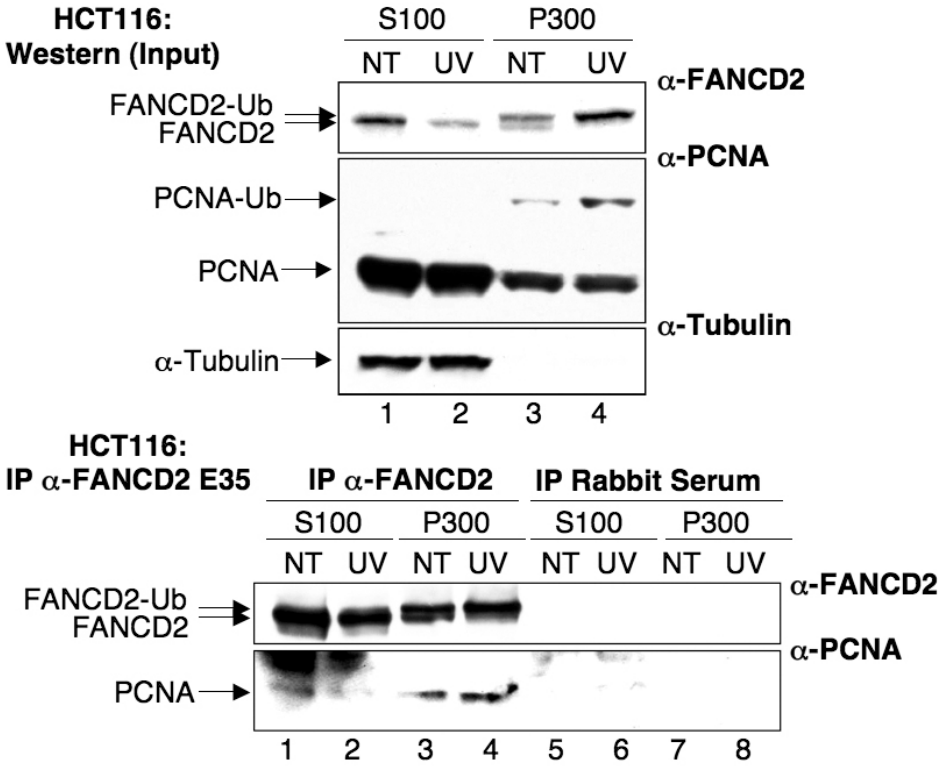
HCT116:
Western (Input)
S100
P300
NT
UV
NT
UV
α-FANCD2
FANCD2-Ub
FANCD2
α-PCNA
PCNA-Ub
PCNA
α-Tubulin
α-Tubulin
1
2
3
4
HCT116:
IP α-FANCD2 E35
IP α-FANCD2
IP Rabbit Serum
S100
P300
S100
P300
NT
UV
NT
UV
NT
UV
NT
UV
α-FANCD2
FANCD2-Ub
FANCD2
α-PCNA
PCNA
1
2
3
4
5
6
7
8

FIGURE S2

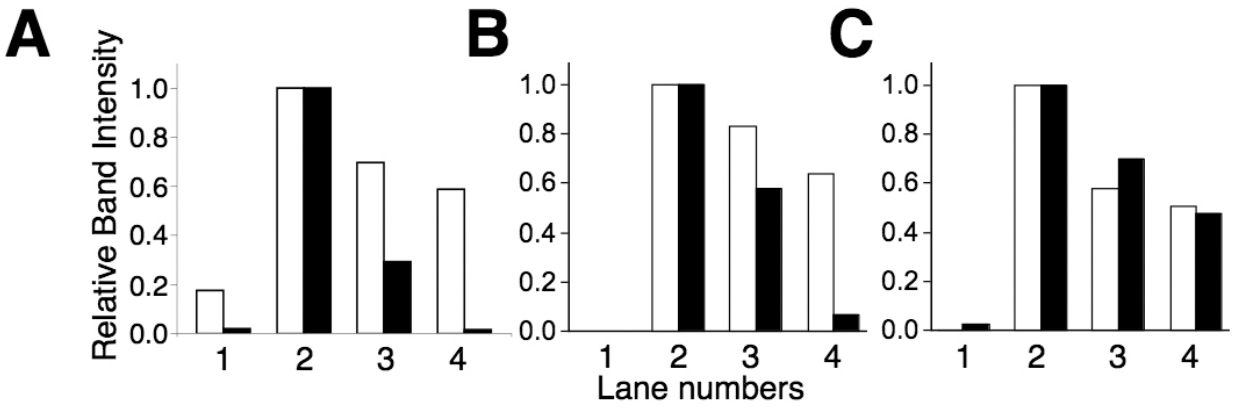
A
B
C
Relative Band Intensity
1.0
0.8
0.6
0.4
0.2
0.0
1
2
3
4
Lane numbers